Mathematical model of skin autofluorescence induced by 450 nm laser

Dmitry N. Artemyev
Samara National Research State University, 34 Moskovskoye shosse, Samara 443086, Russia

e-mail: artemyevdn@gmail.com

Abstract. Optical methods are increasingly being used for the early diagnosis of skin cancer. This approach allows for detecting the component composition changes of tissue in a non-invasive manner. Autofluorescence spectroscopy is a sensitive method for tumor diagnosis and the method availability distinguishes it among other approaches. This work is devoted to fluorescence modeling of skin tissues induced by 450 nm radiation. A multilayer skin model was developed using a set of fluorophores (eumelanin, lipofuscin, riboflavin, beta-carotene, bilirubin) matched with excitation radiation. Model autofluorescence spectra of normal skin tissues of the northern phenotype and pathological changes were obtained. The results were compared with the results of previous experimental studies of *ex vivo* autofluorescence spectra of the skin and neoplasms. © 2018 Journal of Biomedical Photonics & Engineering.

Keywords: Autofluorescence; Monte Carlo Modeling; Skin Model; Skin Fluorophores; Optical Diagnostics.

Paper #3293 received 6 May 2018; revised manuscript received 10 Jun 2018; accepted for publication 16 Jun 2018; published online 30 Jun 2018. doi: 10.18287/JBPE18.04.020303.

References

1. A. D. Kaprin, V. V. Starinsky, and G. V. Petrova, "Malignant Tumors in Russia 2015 (Morbidity and Mortality)," Russia Ministry of health, Moscow (2017) [in Russian]. ISBN 978-5-85502-227-8.
2. V. P. Zakharov, I. A. Bratchenko, D. N. Artemyev, O. O. Myakinin, D. V. Kornilin, S. V. Kozlov, and A. A. Moryatov, "Comparative analysis of combined spectral and optical tomography methods for detection of skin and lung cancers," Journal of Biomedical Optics 20(2), 025003 (2015).
3. I. A. Bratchenko, D. N. Artemyev, O. O. Myakinin, Y. A. Khristoforova, A. A. Moryatov, S. V. Kozlov, and V. P. Zakharov, "Combined Raman and autofluorescence ex vivo diagnostics of skin cancer in near-infrared and visible regions," Journal of Biomedical Optics 22(2), 027005 (2017).
4. H. Lui, J. Zhao, D. McLean, and H. Zeng, "Real-time Raman spectroscopy for in vivo skin cancer diagnosis," Cancer Research 72(10), 2491-2500 (2012).
5. E. Borisova, L. Avramov, P. Pavlova, E. Pavlova, and P. Troyanova, "Qualitative optical evaluation of malignancies related to cutaneous phototype," Proceedings of SPIE 7563, 75630X (2010).
6. I. A. Bratchenko, D. N. Artemyev, O. O. Myakinin, M. G. Vrakova, K. S. Shpuntenko, A. A. Moryatov, S. V. Kozlov, and V. P. Zakharov, "Malignant melanoma and basal cell carcinoma detection with 457 nm laser-induced fluorescence," Journal of Biomedical Photonics & Engineering 1(3), 180–185 (2015).
7. V. V. Tuchin, Tissue Optics, Light Scattering Methods and Instruments for Medical Diagnostics, Third Edition, SPIE, Bellingham (2007). ISBN: 9781628415162.
8. I. V. Meglinski, A. V. Doronin, "Monte Carlo Modeling of Photon Migration for the Needs of Biomedical Optics and Biophotonics," Chap. 1 in Advanced Biophotonics: tissue optical sectioning, 1–72 (2013).
9. A. Yu. Setejkin, I. V. Krasnikov, Application of the Monte Carlo method for biophotonics problems, AmGU publisher, Blagoveshchensk (2014) [in Russian]. ISBN 978-5-93493-224-5.
10. C. Zhu, Q. Liu, "Review of Monte Carlo modeling of light transport in tissues," Journal of Biomedical Optics 18(5), 050902 (2013).
11. A. J. Welch, C. Gardner, R. Richards-Kortum, E. Chan, G. Criswell, J. Pfefer, and S. Warren, "Propagation of fluorescent light," Lasers in Surgery and Medicine 21(2), 166-78 (1997).

12. F. Jaillon, W. Zheng, and Z. Huang, "Beveled fiber-optic probe couples a ball lens for improving depth-resolved fluorescence measurements of layered tissue: Monte Carlo simulations," Physics in Medicine and Biology 53(4), 937–951 (2008).
13. K. B. Sung, H. H. Chen, "Enhancing the sensitivity to scattering coefficient of the epithelium in a two-layered tissue model by oblique optical fibers: Monte Carlo study," Journal of Biomedical Optics 17(10), 107003 (2012).
14. Y. P. Sinichkin, S. R. Utz, A. H. Mavliutov, and H. A. Pilipenko "In Vivo Fluorescence Spectroscopy of the Human Skin: Experiments and Models," Journal of Biomedical Optics 3(2), 201-211 (1998).
15. H. Zeng, C. MacAulay, D. I. McLean, and B. Palcic, "Reconstruction of in vivo skin autofluorescence spectrum from microscopic properties by Monte Carlo simulation," Journal of Photochemistry and Photobiology B: Biology 38(2–3), 234–240 (1997).
16. Q. Liu, C. Zhu, and N. Ramanujam, "Experimental validation of Monte Carlo modeling of fluorescence in tissues in the UV-visible spectrum," Journal of Biomedical Optics 8(2), 223-236 (2003).
17. V. V. Dryemin, Method and device for diagnosis of tissue metabolism disorders based on optical spectroscopy (for example, diabetes mellitus), Diss. Cand. Sci. in Tech., Oryol State University, Oryol, Russia, 2017 [in Russian].
18. I. V. Meglinski, S. J. Matcher, "Computer simulation of the skin reflectance spectra," Computer Methods and Programs in Biomedicine 70(2), 179-186 (2003).
19. S. L. Jacques, "Optical properties of biological tissues: a review," Physics in Medicine and Biology 58(11), R37–R61 (2013).
20. A. N. Bashkatov, E. A. Genina, and V. V. Tuchin, "Optical properties of skin, subcutaneous, and muscle tissues: a review," Journal of Innovative Optical Health Sciences 4(1), 9–38 (2011).
21. E. G. Borisova, L. P. Angelova, and E. P. Pavlova, "Endogenous and Exogenous Fluorescence Skin Cancer Diagnostics for Clinical Applications," IEEE Journal of Selected Topics in Quantum Electronics 20(2), 211–222 (2014).
22. K. Koenig, I. Riemann, "High-resolution multiphoton tomography of human skin with subcellular spatial resolution and picosecond time resolution," Journal of Biomedical Optics 8(3), 432 (2003).
23. A. C. Croce, G. Bottiroli, "Autofluorescence spectroscopy and imaging: a tool for biomedical research and diagnosis," European Journal of Histochemistry 58(4), (2014).
24. S. P. Nighswander-Rempel, J. Riesz, J. Gilmore, J. P. Bothma, and P. Meredith, "Quantitative Fluorescence Excitation Spectra of Synthetic Eumelanin," Journal of Physical Chemistry B 109(43), 20629-20635 (2005).
25. M. E. Darvin, I. Gersonde, M. Meinke, W. Sterry, and J. Lademann, "Non-invasive in vivo determination of the carotenoids beta-carotene and lycopene concentrations in the human skin using the Raman spectroscopic method," Journal of Physics D: Applied Physics 38(15), 2696–2700 (2005).
26. V. D. Silva, J. N. Conceição, I. P. Oliveira, C. H. Lescano, R. M. Muzzi, O. P. S. Filho, E. C. Conceição, G. A. Casagrande, and A. R. L. Caires, "Corrigendum to 'Oxidative Stability of Baru (Dipteryx alataVogel) Oil Monitored by Fluorescence and Absorption Spectroscopy," Journal of Spectroscopy 2015, 748673 (2015).
27. B. Thorell, "Flow-cytometric monitoring of intracellular flavins simultaneously with NAD(P)H levels," Cytometry 4(1), 61–65 (1983).
28. D. M. Gore, P. French, D. O'Brart, C. Dunsby, and B. D. Allan, "Two-Photon Fluorescence Microscopy of Corneal Riboflavin Absorption Through an Intact Epithelium," Investigative Ophthalmology & Visual Science 56(2), 1191–1192 (2015).
29. B. Zietz, A. N. Macpherson, and T. Gillbro, "Resolution of ultrafast excited state kinetics of bilirubin in chloroform and bound to human serum albumin," Physical Chemistry Chemical Physics 6(19), 4535 (2004).
30. N. Nandakumar, S. Buzney, and J. J. Weiter, "Lipofuscin and the Principles of Fundus Autofluorescence: A Review," Seminars in Ophthalmology 27(5–6), 197–201 (2012).
31. N. M. Haralampus-Grynaviski, L. E. Lamb, C. M. R. Clancy, C. Skumatz, J. M. Burke, T. Sarna, and J. D. Simon, "Spectroscopic and morphological studies of human retinal lipofuscin granules," Proceedings of the National Academy of Sciences 100(6), 3179–3184 (2003).
32. A. Periasamy, and R. M. Clegg, Flim Microscopy in Biology and Medicine, CRC Press, Taylor & Francis Group, Boca Raton (2009). ISBN 9781420078909.
33. G. F. M. Ball, "Flavins: Riboflavin, FMN and FAD (Vitamin B2)," Chap. 12 in Vitamins: Their Role in the Human Body, 289–300 (2008).
34. R. L. Barnhill, M. Piepkorn, and K. J. Busam, Pathology of Melanocytic Nevi and Malignant Melanoma, Springer, Berlin (2004). ISBN 978-0-387-21619-5.
35. A. A. Efimov, G. N. Maslyakova, "Lipofuscin role in involutive and pathological processes," Saratov Journal of Medical Scientific Research 5(1), 111-115 (2009) [in Russian].
36. A. Skoczyńska, E. Budzisz, E. Trznadel-Grodzka, and H. Rotsztejn, "Melanin and lipofuscin as hallmarks of skin aging," Advances in Dermatology and Allergology 2, 97–103 (2017).

37. P. A. van den Berg, J. Widengren, M. A. Hink, R. Rigler, and A. J. W. Visser, "Fluorescence correlation spectroscopy of flavins and flavoenzymes: photochemical and photophysical aspects," Spectrochimica Acta Part A: Molecular and Biomolecular Spectroscopy 57(11), 2135–2144 (2001).
38. A. Dontsov, A. Koromyslova, M. Ostrovsky, and N. Sakina, "Lipofuscins prepared by modification of photoreceptor cells via glycation or lipid peroxidation show the similar phototoxicity," World Journal of Experimental Medicine 6(4), 63 (2016).
39. A. Hennessy, C. Oh, B. Diffey, K. Wakamatsu, S. Ito, and J. Rees, "Eumelanin and pheomelanin concentrations in human epidermis before and after UVB irradiation," Pigment Cell Research 18(3), 220–223 (2005).
40. D. L. Fox, Biochromy, Natural Coloration of Living Things, University of California Press, Berkley and Los Angeles (1979). ISBN 0-52003699-9.
41. A. Vahlquist, J. B. Lee, G. Michaëlsson, and O. Rollman, "Vitamin A in Human Skin: II Concentrations of Carotene, Retinol and Dehydroretinol in Various Components of Normal Skin," Journal of Investigative Dermatology 79(2), 94–97 (1982).
42. A. Knudsen, R. Brodersen, "Skin colour and bilirubin in neonates," Archives of Disease in Childhood 64(4), 605–609 (1989).
43. I. A. Novikov, Y. O. Grusha, and N. P. Kiryshchenkova, "Autofluorescence diagnostics of skin and mucosal tumors," Annals of ophthalmology 129(5), 147-153 (2013).
44. K. S. Litvinova, D. A. Rogatkin, O. A. Bychenkov, and V. I. Shumskiy, "Chronic Hypoxia as a Factor of Enhanced Autofluorescence of Endogenous Porphyrins in Soft Biological Tissues," Proceedings of SPIE 7547, 75470D (2010).
45. M.-A. Mycek, B. W. Pogue, Handbook of biomedical fluorescence, Marcel Dekker Inc., New York (2003). ISBN: 0824709551
46. K. Konig, H. Meyer, and H. Schneckenburger, "The Study of Endogenous Porphyrins in Human Skin and Their Potential for Photodynamic Therapy by Laser Induced Fluorescence Spectroscopy," Lasers in Medical Science 8, 127-132 (1993).
47. E. Borisova, P. Pavlova, E. Pavlova, P. Troyanova, and L. Avramov, "Optical Biopsy of Human Skin – A Tool for Cutaneous Tumours' Diagnosis," International Journal Bioautomation 16(1), 53-72 (2012).

1 Introduction

Skin cancer is one of the most common forms of cancer in Russia and the world [1]. There are three main types of skin cancer: basal cell carcinoma (BCC), squamous cell carcinoma (SCC) and malignant melanoma (MM). Optical methods have been extensively used to diagnose neoplasms, since they are non-invasive and can be applied to real-time analysis [2-4]. One of the promising methods of non-invasive skin lesion examination is the analysis of the tissue intrinsic fluorescence. Laser induced autofluorescence (AF) spectroscopy is an effective method for early detection of skin cancer because of its high sensitivity, simple measurement technique, and the absence of contrast agents in the studied tissue [5]. Economic efficiency of AF spectroscopy for cancer diagnosis is an important factor in the possible use of the method in clinical studies.

The empirical analysis allows for distinguishing the diseased tissue, but in many cases, it is impossible to establish a clear connection between the final cancer diagnosis and biochemical changes in malignant tissues. For example, the registered fluorescence spectrum can be analyzed to determine the spectral contributions of constituent components to obtain the concentration of individual fluorophores. Nevertheless, the tissue is a multi-scattering medium, and fluorescence depends on various factors: the concentration of fluorophores, their localization, scattering and absorption of other chromophores, the geometry of the excitation / collection probe, and others. These effects can distort the shape of the spectrum and radiation intensity. For example, significantly altered AF spectra will be recorded for two skin tissues samples of different phenotypes with the same composition and concentration of fluorophores, due to the absorbing properties of melanin.

A proper measurement evaluation of fluorescence intensity in healthy tissue and pathology areas will be possible if the penetration depth of the probing radiation is known. This fact would provide information about fluorophores and blood vessels (upper or deep plexus of blood vessels) involved in the signal shaping.

Recent advances in computer modeling are an essential tool for studying the biological basis of the registered signals in the fluorescence studies. They contribute to better identification of important fluorophores present in specific tissues. The purposes of the study are qualitative assessment, modeling the autofluorescence spectral characteristics changes of healthy skin and tumors induced by 450 nm laser, and obtained results comparing with a previously experimentally registered AF spectra within this range [3, 6].

2 Modeling methods of skin autofluorescence

2.1 Modeling the light in tissues by Monte Carlo method

The mathematical description of light absorption and scattering characteristics may be performed in two ways: using analytical theory or radiation transfer theory (RTT). The analytic theory is based on the Maxwell equations and is the most fundamental approach. However, its use is limited by difficulty of accurate analytical solutions obtaining. On the other hand, the radiation transport theory estimates the transfer of photons through absorbing and scattering media, without considering Maxwell's equations. The RTT is widely used to describe the interactions of optical radiation in tissue. It has been experimentally confirmed in many cases that RTT predictions are sufficient [7-9].

The stationary equation of the radiation transfer theory for monochromatic light is studied in details in the book [7]. It describes the average power change of the flux density at a certain point and in a certain direction, taking into account the scattering properties of the medium. The main challenge of RTT is diffuse component definition of the beam intensity, since scattering of photons is random. Therefore, different approximations are used, according to the intensity change is caused by the absorption or scattering of light.

Several approximation classes have been proposed in recent decades, including analytical models based on the theory of probabilistic photon migration, Kubelka-Munk theory, diffusion approximation theory, and a combination of various analytical methods. The advantage of analytical models is a relatively simple form of solution, but specified boundary conditions are required. Alternative approaches are various modifications of the Monte Carlo method. It is able to take into account the probe geometry and the complex structure of the tissue. However, this method requires relatively high processing power.

Radiation transport in tissues is modeled by the steps tracking of photon random walk using the Monte Carlo (MC) method [10]. To simulate fluorescence, an additional parameter – the quantum yield is included to describe the probability that an absorbed photon can be converted to a fluorescent photon at a different wavelength [11]. The initial direction of the fluorescent photon is isotropic due to the nature of the fluorescent radiation. The absorbing and scattering properties of the tissue model will influence on the fluorescence intensity in addition to the quantum yield and lifetime. Fluorescence modeling is usually more time consuming task than simulating diffuse reflection due to the additional propagation of fluorescent photons.

The most common application of the MC method in tissue optics is the modeling of optical measurements, such as diffuse reflection, transmittance and fluorescence for a given tissue model and the geometry of illumination / collection probe [12, 13].

2.2 Review of Monte Carlo models of skin autofluorescence in the visible region

It is useful to consider the basic approaches of the MC models construction for AF spectrum registration of skin on the example of the following works. Ref. [14] presented the results of an experimental study of the autofluorescence spectra of human skin *in vivo* induced by UV radiation (337 nm) and external mechanical pressure applied to the skin. These results were compared with the results of Monte Carlo simulation of the skin autofluorescence with various blood content. The proposed skin model made it possible to evaluate changes in the blood and melanin content. The skin model consisted of four layers. The fluorescent properties of the model were determined by melanin, hemoglobin, and collagen. In fact, collagen was only chosen as the fluorophore, melanin and hemoglobin were absorbers in the path of the AF signal. In this model, the authors ignored epidermal fluorescence because of the low contribution of fluorescent photons passing through the dermis.

The contribution of each layer to the AF spectrum of skin registered *in vivo* was shown in Ref. [15]. A standard seven-layer model (stratum corneum, epidermis, papillary dermis, upper vascular plexus, reticular dermis, deep plexus of vessels, dermis) was used. The AF spectra for each layer were registered using a microscope and excited laser with a wavelength of 442 nm. The contribution of each layer to the resulting skin AF spectrum was assessed in the simulation, rather than the effect of individual fluorophores.

The effect of individual fluorophores on the final AF spectrum was demonstrated in Ref. [16]. The aim of the work was experimental confirmation of MC fluorescence modeling in turbid phantom models. A simulation of the absorption and scattering coefficients effect on fluorescence of a turbid medium was carried out. The phantom skin model consisted of three components: two fluorophores (flavin adenine dinucleotide and green fluorescent protein) and one absorber (India ink). The excitation wavelength of 460 nm was matched with the excitation maxima of both fluorophores. Optical properties and the quantum yield of fluorescence measured on tissue phantoms were experimentally obtained to MC simulation. The results of MC simulation showed a good agreement between the model and experimentally measured results.

In another paper on the AF modeling of tissue using a fiber-optic sensor [17], real skin fluorophores have been used. Fluorescence was excited by 450 nm radiation. NADH and collagen were chosen as fluorophores, although their excitation peak was shifted to the shorter wavelength range of 330-340 nm. The multilayer skin model included: stratum corneum, epidermis, papillary dermis, reticular dermis and was

implemented in the optical modeling system TracePro. The effect of melanin on the AF spectrum was also taken into account.

In the reviewed models, the choice of fluorophores was not obvious and modeling of the skin pathological stages was not performed. A detailed analysis of the possible skin components (fluorophores and chromophores) for modeling and their spectral characteristics are described in the following paragraphs.

3 Multilayer skin model for autofluorescence induced by 450 nm laser

Highlights were taken into account in constructing of skin AF model (a set of layers, fluorophores) based on an analysis of existing models and the literature. A wavelength of 450 nm was chosen to excite AF and compare the model results with experimentally registered AF of skin and neoplasms. The modeling environment was TracePro Expert - 6.0.2, Lambda Research Corporation. Multilayer skin model was designed. The main difference of the proposed model was a set of fluorophores for skin AF modeling induced by 450 nm radiation. The features of the absorption spectra (the maximum value located in the range 440-460 nm) determined the choice of each fluorophore.

To obtain a fluorescent response, human skin was represented as a model consisting of five planar layers: epidermis, papillary dermis, upper plexus of microvessels, reticular dermis and deep vascular plexus [7, 18]. The thickness of individual skin layers: the epidermis – 100 μm, the papillary dermis – 200 μm, the surface plexus of microvessels – 100 μm, the reticular dermis – 600 μm and the deep plexus of the vessels – 200 μm. To simulate AF the skin area was selected with the size of 40 mm × 40 mm.

The optical characteristics of individual layers were repeatedly studied [7, 14, 15, 19, 20]. The absorption and scattering coefficients, anisotropy and refractive indices of each layer for normal skin and neoplasms were presented in the book [7]. It is also necessary to set the following parameters for fluorescence modeling: 1) quantum yield, 2) molar extinction coefficient, 3) molar concentration, 4) excitation spectra, 5) emission spectra. The values of relative absorption, excitation, and emission must be normalized to import data in the TracePro environment.

Since the fluorescent properties of the skin are determined by the fluorescent properties of the fluorophores contained in layers, the choice of components is a key moment in the modeling of the skin AF signal. Most studies to detect and evaluate AF signals of skin and neoplasms are performed using radiation in the spectral range of 330-450 nm [21]. The excitation spectra of most endogenous fluorophores, such as structural proteins, coenzymes, pigments, endogenous porphyrins, are located in this spectral range. Excitation in the 280-330 nm region was used to study amino acids such as tryptophan and tyrosine. Their fluorescent signal is correlated with the tissue health. Endogenous fluorophores were chosen with an absorption maximum in the 440-460 nm region, which play an important role in the formation of fluorescent properties of normal and pathological skin tissues, based on the analysis of spectral characteristics (excitation and emission spectra). Spectral data and fluorescent properties (quantum yield, peak of molar extinction) were selected according to the analysis of review articles on the skin intrinsic fluorescence [21-23], and papers devoted to the investigation of individual skin components fluorescence [24-31]. Part of the spectral data was obtained using the OMLC web resource (https://omlc.org/index.html), which provides databases, software, articles and free web guides on biomedical optics, supported by Scott Prahl and Steven Jacques. The following fluorophores were chosen to the designed model: melanin (absorption range of 250-1100 nm), carotenoids (absorption range of 400-550 nm with maximum values at 440 and 480 nm), flavins (absorption range of 300-500 nm with maximum values at 370 and 445 nm), bilirubin (absorption range of 300-600 nm with a maximum value of 450 nm) and lipofuscin (absorption range of 430-600 nm with a maximum value of 480 nm).

3.1 Skin fluorophores

Each fluorophore is discussed in detail in the presented model. Melanin is a high molecular weight pigment that is synthesized in specialized cells called melanocytes, which are located in the basal cell layer [32].

Carotenoids are natural organic pigments of yellow, orange or red color. Carotenoids are antioxidants in the human body that come with nutrition. Natural sources of carotenoids are a mixture of lycopene, beta-carotene, alpha-carotene, lutein, and zeaxanthin, which can be converted into each other. Beta-carotene was chosen as an example of carotenoids in the model. It is one of the chromophores of the upper dermis layers [20, 25].

Flavins are complex enzymes, the prosthetic groups of which are riboflavin derivatives [33]. Riboflavin is a biologically active substance that plays an important role in health support. The biological role of riboflavin is determined by the occurrence of its derivatives: flavin mononucleotide (FMN) and flavin adenine dinucleotide (FAD), which are part of a large number of important oxidation-reduction enzymes as coenzymes. In the skin, flavins are located in the basal layer and dermis [32].

Bilirubin is a bile pigment, one of the main components of bile in humans and animals. It is formed normally as a result of the proteins cleavage containing heme: hemoglobin, myoglobin, and cytochrome. Hemoglobin exhibited absorbing properties and contained in the dermis and blood [20].

Lipofuscin is a yellow-brown, intracytoplasmic autofluorescent pigment, consisting of a glycolipoprotein matrix, it contains in all tissues and organs of human [34]. Lipofuscin is also called aging pigment, which accumulates in the skin with age. But,

the accumulation of lipofuscin can be associated with pathological processes in the body [35]. Lipofuscin has similar properties to melanin for dermatology specialists, but lipofuscin has a more intense fluorescent response [34, 36]. Lipofuscin was considered as a fluorophore in the modeling of non-melanoma neoplasms.

Based on the above-described data of fluorophores, the fluorescent properties of the epidermis were characterized by eumelanin located in the lower part of the layer. The fluorescent properties of the dermis are determined by beta-carotene and flavins localized in the upper and lower layers, respectively. The fluorescent properties of the dermis with superficial plexus of vessels were characterized by bilirubin. Lipofuscin in the modeling of the skin pathologies was placed in the upper layer of the epidermis. In the simulation of pigmented tumors (malignant melanoma) eumelanin with fold increased content was localized in the upper layers of the epidermis. The final distribution of fluorophores over the skin layers in the model is shown in Fig. 1.

To simulate fluorescence, the fluorescent properties of the components were set: the quantum yield, the peak of molar extinction. In addition to fluorescent properties, a possible fluorophore concentration in the skin was determined. The parameters of the fluorophores used in the model are presented in Table 1 [24, 29, 31, 37, 38].

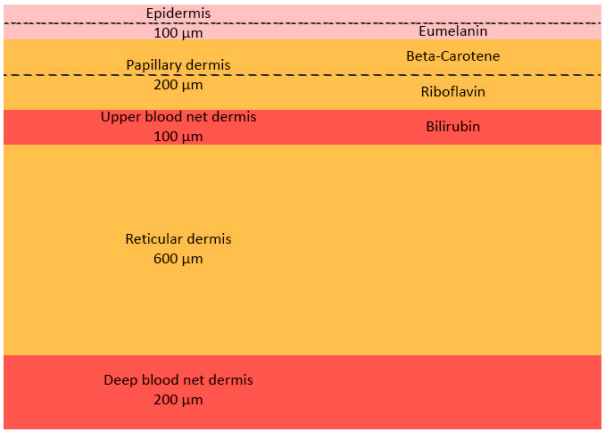

Fig. 1 Fluorophores localization in the multilayer model of healthy skin.

Table 1 Fluorescent properties of skin components.

Fluorophore	Quantum yield, γ	Peak of molar extinction, ε [l/mol·cm]	Molar concentration, C_{mol}, [mol/l]	Absorption coefficient, μ_a [cm^{-1}]
Eumelanin	0.0004	2500-3000	$0.88 \cdot 10^{-2}$	10
Lipofuscin	0.01	31 000	10^{-3}	23.6
Riboflavin (Flavins)	0.26	13 153	$6.4 \cdot 10^{-5}$	0.4
Beta-Carotene (Carotenoids)	0.0001	138 590	$2.3 \cdot 10^{-5}$	2.6
Bilirubin	0.003	55 016	$1.9 \cdot 10^{-4}$	10.5

The molar concentrations of fluorophores characteristic for the skin were taken from Refs. [38-42]. The table indicates that the absorption coefficient, which is directly proportional to the product of the molar concentration and the peak of the molar extinction, takes the highest values for eumelanin, lipofuscin and bilirubin. These components are mainly responsible for the absorption of radiation. Taking into account the quantum yield of fluorophores, the fluorescent contribution of each of them was estimated. Flavins and lipofuscin exhibit the strongest fluorescent properties.

3.2 Model of the optical scheme for skin fluorescence registration

The common optical scheme was used for registration of the skin fluorescent response. The scheme is shown in Fig. 2.

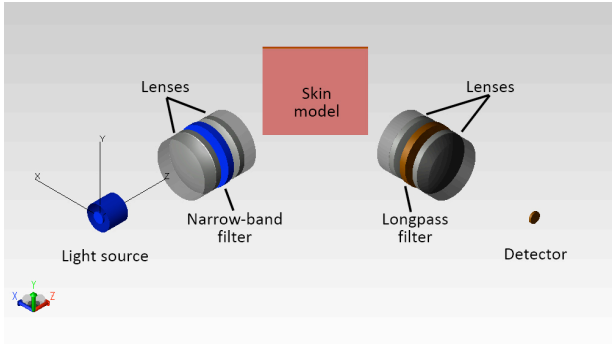

Fig. 2 Model of the optical scheme for skin fluorescence registration.

This optical scheme is standard for registration of samples fluorescence in TracePro. It consists of a detector, two focusing systems and a light source at 450 nm with a deflector for less scattering of rays. Each focusing system includes two lenses and a filter. The focusing system, which is closer to the source, is a

monochromator and serves to extract the radiation with a narrow wavelength. The second focusing system contains a longpass filter to suppress the probe radiation. The transmission and absorption characteristics of the filters elements and optical glass were matched for a wavelength of 450 nm (narrow-band filter - FF01-448/20, longpass filter - Di02-R442). The light source and the detector are perpendicular to each other to prevent the detector illuminating by the scattered radiation from the source.

4 Results and discussion

The depth of radiation penetration with a wavelength of 450 nm was initially analyzed in our model. This fact should be reviewed since the results of model experiments in published papers [15, 17] were applied for a combination of layers or for a limited set of fluorophores, respectively. The simulation results are shown in Fig. 3, each point corresponds to the average value of the radiation power at the upper boundary of each layer. The figure indicates that only 11% of the initial value (average power at the upper border of the epidermis) remains at the upper boundary of the reticular dermis (400 μm). And only 4% of radiation power falls on the layer with the deep plexus of the vessels. It follows that the main part of the incident radiation flux is localized in the three upper layers of the skin to 400 μm (epidermis, papillary dermis, surface plexus of vessels) in which the fluorophores under consideration are located. The obtained dependence is well correlated with the results of modeling in [15, 17]. In the work of Zeng group [15] the fluorescent properties of each layer were set by experimentally registered spectra and the propagation of 442 nm radiation was simulated. The main part of the radiation decayed to 300 μm, and at a depth of 570 μm, radiation was practically absent. In Ref. [17], radiation with a wavelength of 450 nm was also concentrated in the upper layers, the depth reached 450-500 μm and penetrated into the epidermis, the papillary dermis and captured the upper vascular plexuses. At the same time, the results of MC modeling were confirmed by analytical calculations, the difference was not more than 5%.

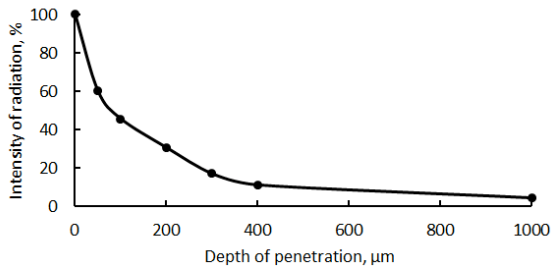

Fig. 3 The average power dependence of the incident radiation with a wavelength of 450 nm from the penetration depth in the skin model.

The main task of this work was skin model development using matched fluorophores for comparison with the experimental AF spectra of skin and neoplasms induced by 457 nm laser [6]. In Ref. [6], the analyzed spectral range of the registered values was shifted to the long-wavelength region relative to the excitation wavelength. Therefore, the AF response was modeled in the range of 540-720 nm for comparison with the experimental results. The signal in the near-IR region (720-750 nm) was not considered, since the last two intensity values (690 and 715 nm) were close to zero. The multilayer skin model was developed for the northern phenotype (concentration of eumelanin in the lower layer of the epidermis was $0.88 \cdot 10^{-2}$ mol/l). To model lesions in the skin model, the additional fluorophore was localized in the upper layers of the epidermis. For "tumor" model lipofuscin concentration was $0.4 \cdot 10^{-3}$ mol/l, for malignant melanoma the concentration was 10^{-1} mol/l. The simulation results are shown in Fig. 4.a, which are compared with the characteristic experimental AF spectra of basal cell carcinoma, malignant melanoma and healthy skin (Fig. 4.b).

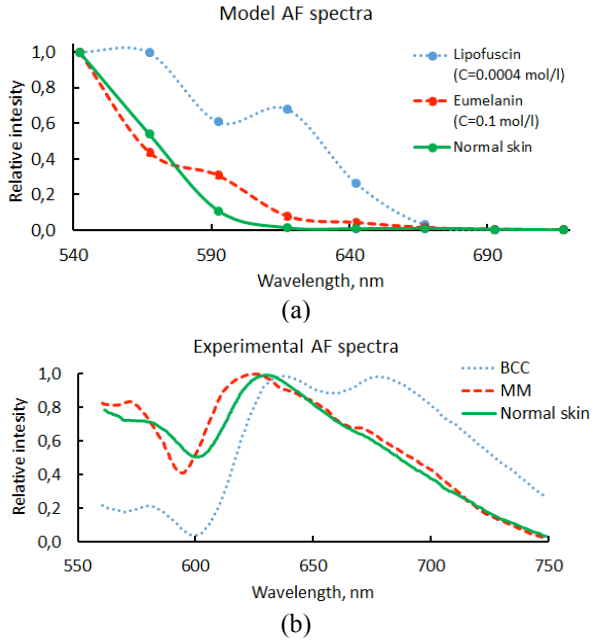

Fig. 4 Normalized model AF spectra of normal skin, tumor (lipofuscin) and malignant melanoma (eumelanin) for the northern phenotype (a) and experimental AF spectra of healthy skin, basal cell carcinoma and malignant melanoma (b).

Despite the small number of points, the figure highlights the characteristic common features: the relative intensity increase of the "tumor" AF signal in comparison with normal skin and "MM"; displacement of the "tumor" maximum in the long-wave region (620-640 nm); the presence of two characteristic peaks in the "tumor" spectrum (560 and 625 nm); a close arrangement for normalized spectra of normal skin and "MM". As was shown in Ref. [6], the positions and the maxima intensities of the AF spectra can provide information on the chemical composition of the examined samples. Thus, these features indicate the

changes in the pathological neoplasms compared to healthy skin. The main fluorophores emitting in the spectral range 550-700 nm are lipopigments, flavins and porphyrins [43, 44]. Lipids and flavins form the peak in the region 570-590 nm. Lipopigments have an absorption maximum at 340 nm and an emitting maximum at 560 nm. Flavins are characterized by strong absorption in a wide range from 200 to 500 nm with strong absorption maxima at 220, 260 nm, less absorption at 380, and 460 nm. The maximum intensity of flavin emission is located in a band centered at 555 nm [45]. Porphyrins are characterized by wide absorption in the region of 300-470 nm with a maximum value in the 400-410 nm band. The emission of porphyrins has a complex shape with two maxima around 615-630 and 660-670 nm [43, 44, 46]. Thus, the local maximum of AF spectra observed for the 560-570 nm band is characterized by the presence of flavins and lipopigments in the skin tissues, and the porphyrins determine the shape of the AF spectra in the red region of the spectrum.

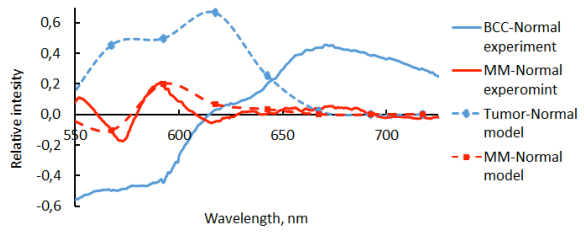

Fig. 5 The intensities changes of neoplasms normalized AF spectra relative to normal skin in model (dashed line) and experimental studies (solid line).

In this study, it was important to determine the fluorophores responsible for the intensity changes of the neoplasms AF spectra compared to normal skin. To analyze these dependence, normal skin spectrum was subtracted from the values of the neoplasms intensities for modeling and experimental study. Before subtraction, the experimental values were shifted to the shortwave region by 15 nm due to the calibration of the spectrometer. The obtained dependence of the AF spectra intensities changes is shown in Fig. 5. Fig. 5 indicates good qualitative agreement of the model results for normal skin and MM AF spectra with the experimental results. The greatest changes of the intensities were characteristic for the 580-600 nm band in both cases. The difference in the intensities of the normalized spectra in this band in the model and in the experiment does not exceed 20%. And the largest deviations of model values from the experiment do not exceed 10% over the entire spectral range. The modeling results of intensities change for tumor relative to normal skin are in poor agreement with experiment. For model values of AF tumor spectra, an increased intensity in the range of 550-640 nm was characteristic, and an inverse trend was observed for the BCC experimental study. This result figures out that model tumor can not be a BCC. The increased values of AF intensity in comparison with normal skin for the examined area are characteristic for squamous cell carcinoma [47].

The shape of the AF spectra differs between the model and the experiment. This is primarily due to the limited number of fluorescence sources (points on the abscissa axis) and an incomplete set of fluorophores. The model did not consider fluorophores whose absorption maxima do not locate within the 440-460 nm band. However, the part of radiation can be absorbed by fluorophores and re-emitted in the considered spectral range. Porphyrin is a fluorophore that can make significant changes to the model AF spectrum. This fluorophore was not presented in the model due to the shift of the absorption maximum to the short-wave region of the spectrum (400-410 nm).

The simulation results confirmed the differences of the pathology spectra in comparison with healthy tissue may be caused by different concentrations of melanin, flavins and lipopigments, while bilirubin and carotenoids do not significantly change the model spectrum.

5 Conclusion

The multilayer model of skin and pathologies using fluorophores (melanin, carotenoids, flavins, bilirubin and lipofuscin) was proposed. The fluorophores were matched with an excitation wavelength of 450 nm.

Model AF spectra of healthy skin and neoplasms were obtained. Because of the large number of simulation events (each count on the abscissa axis is essentially an independent source of fluorescence), the number of points in the model spectrum (540-715 nm) was limited. Thus, the analysis of the AF spectrum was carried out in specific positions with a step of 25 nm. For the considered positions, the intensities difference for the model spectra of the “malignant melanoma” and the normal skin had a good qualitative agreement with the experimental results. Higher values of intensities were obtained for the malignant formations in the long-wavelength region of the spectrum (550-640 nm) which are characteristic for squamous cell carcinoma. The presence of characteristic peaks in the model spectrum is primarily determined by flavins and lipopigments. And an increased concentration of lipopigments may indicate the pathological changes.

Disclosures

The author declares that there is no conflict of interests in this paper.

Acknowledgments

This research was supported by the Ministry of Education and Science of the Russian Federation.